Environmental Science and Pollution Research
https://doi.org/10.1007/s11356-023-26822-8

Bio-adsorbent hydroxyapatite for drinking water defluoridation: column performance modelling studies

Dhiraj Mehta[1] · **Virendra Kumar Saharan**[1] · **Suja George**[1]

Received: 9 January 2023 / Accepted: 31 March 2023

Abstract

Waste marble powder (WMP) is a rich source of calcium and magnesium salts having an affinity for fluoride ions and therefore serves as a good defluoridation agent. Hydroxyapatite was synthesized from WMP generated by the marble processing industry to make an adsorbent for drinking water defluoridation. The synthesized marble hydroxyapatite (MA-Hap LR) powder was further formed into 2–3 mm pellets by extrusion spheronization technique using a polyvinyl alcohol binder. Continuous column defluoridation studies were conducted to obtain optimized column parameters such as input fluoride concentration, column inflow rates, optimum pellet size, and adsorbent bed parameters to obtain maximum fluoride adsorption capacity. The best breakthrough column performance was a maximum adsorption capacity of 1.21 mg/g, treating 10 mg/L fluoride concentration. The optimized column flow rate was at 1 LPH using an adsorbent bed height of 25 cm, which processed 28.5-bed volumes at an adsorbent exhaustion rate of 7.4 g/L. The column breakthrough performance data were fit into various kinetic models (Thomas model and Yoon–Nelson model) to describe adsorption kinetics and obtain correlation coefficients. Thomas's model fitted well with a high correlation coefficient value. Modelling studies indicate MA-Hap as a promising adsorbent for drinking water treatment, and optimum column design parameters were identified for scale-up for real applications.

Keywords Fluoride · Adsorption · Continuous column studies · Modelling · Hydroxyapatite · Waste marble powder

Introduction

The marble processing operations generate vast marble waste powder in the slurry/powder form (Khan et al. 2020). Indiscreet disposal of these into the environment is a significant cause of concern as it affects the air, water, and soil environment. Calcium and magnesium compounds are significantly present in marble waste powder (WMP) in the form of dolomite ($CaMg(CO_3)_2$), calcite ($CaCO_3$), and silicon oxides (Segadães et al. 2005). It can be used as a raw material to synthesize hydroxyapatite (Hap), a promising adsorbent for fluoride removal in drinking water (Mehta et al. 2016; Singh et al. 2020). Groundwater contamination with fluoride has become a burning issue and of significant concern due to its hazardous effects (Zendehdel et al. 2022) such as dental and skeletal fluorosis, a degenerative bone disease causing deformities in children and adolescents, and disorders in pregnant and lactating mothers (Singh et al. 2018). The adsorption process is the most commonly accepted and efficient method in drinking water treatment because it is low-cost, easily available, easy operation, and eco-friendly (Li et al. 2022; Yadav et al. 2022). Green, environmentally friendly adsorbents, such as Hap, based on calcium compounds, have gained interest in drinking water treatment in the past two decades. It is safer to use than metal-based adsorbents that have the probability of dissolving into the treated water with variations in the pH/alkalinity of the water. Calcium being nontoxic and biocompatible, calcium-based materials can serve as adsorbents as the permissible limit of calcium in drinking water is as high as 7×10^{-2} g/L and can reach up to 2×10^{-1} g/L in the absence of sufficient/reliable water source. Few medical studies, especially in children, indicate the feasibility of treating and reversing fluorosis through calcium intake (George et al. 2021). Hap is the main constituent of human and animal teeth and

Responsible Editor: Tito Roberto Cadaval Jr

✉ Suja George
sgeorge.chem@mnit.ac.in

[1] Malaviya National Institute of Technology, Jaipur 302017, India

Published online: 11 April 2023

bone. Its biocompatible and environmentally friendly nature attracts attention due to its unique apatite structure (Liang et al. 2011). Synthetic Hap possesses a higher defluoridation capacity (Khan et al. 2020; Scheverin et al. 2022). Synthetic Hap can be produced from WMP using various processes such as the conventional sol–gel precipitation, hydrothermal process, or chemical precipitation method. The nature of the synthesized Hap product is highly process dependent, and different kinds of crystalline structures such as plate-like (Méndez-Lozano et al. 2022), spherical-shaped (Mehta et al. 2018) elongated nanorods (Mehta et al. 2017) and nanoparticles have been reported. The fluoride adsorption capacity of Hap is affected by calcination. It has been reported that uptake capacity of un-calcined HAP was found to be 4.38 mg F/g HAP. In contrast, it was 3.53 mg/g for HAP calcined at 300 °C and further reduced to 0.7 mg/g for HAP when calcined at 800 °C (Singh et al. 2020). The synthesis of Hap by the gel precipitation method is the most commonly used because of the low-cost, eco-friendliness, process simplicity, and applicability in industrial production (Mohd Pu'ad et al. 2019), (Khan et al. 2022).

The comparative study on the batch fluoride adsorption capacity of MA-Hap powder synthesized from waste marble powder by the conventional gel precipitation method (MA-Hap CM), ultrasonication (MA-Hap USM), and pilot plant lab reactor (MA-Hap LR) has been reported by the author group along with their energy efficiency and synthesis costs (George et al. 2022). The various grades of pure MA-Hap powder had a batch fluoride removal capacity varying from 1.33 to 1.826 mg/g at neutral pH for an adsorbent dose of 5.0 g/L treating 10 mg/L fluoride water, within an equilibrium contact time of 30 min. The adsorption isotherm and kinetics for MA-Hap followed the Langmuir model and pseudo-second-order kinetics, respectively. The adsorption capacity of pure and modified synthetic Hap can be increased using various reagents during process synthesis (Khan et al. 2020). The lowest adsorption capacity of Hap at 0.489 mg/g was reported by Sairam Sundaram et al. (2009) using reagents such as calcium nitrate, ammonium dihydrogen phosphate, and (NH4)2-EDTA complex in synthesis, whereas the highest capacity of 40.818 mg/g was reported by Zhang et al. (2012) when Hap was synthesized using phosphogypsum, diammonium phosphate, and sodium hydroxide. As the study indicated that MA-Hap adsorbent had good potential for defluoridation, this work, therefore, focuses on the study of column adsorption capacity of MA-Hap pellets prepared from MA-Hap powder by the extrusion–spheronization technique.

The fluoride adsorption performance of Ma-Hap LR pellets has been studied in packed bed columns and investigated for their practical feasibility, along with adsorber column design parameters that can be useful for field applications. This study presents the modelling of adsorption kinetics and the design of adsorption column parameters to obtain maximum fluoride adsorption capacity. No paper has reported the modelling of breakthrough curves of fluoride adsorption performance of marble waste-derived hydroxyapatite pellets in the defluoridation of drinking water. The practical applicability of MA-Hap pellets for real applications in the defluoridation of drinking water was studied.

Materials and methods

Analytical grade chemicals were used to prepare standard solutions for fluoride analysis in water samples. Marble waste powder (WMP) was collected from the marble processing industries of Kishangarh, located in Rajasthan, India. A fully controlled pilot plant scale reactor (capacity of 60 L) was used to synthesize marble hydroxyapatite by the gel precipitation process at an optimized reaction temperature of 72 °C. Initially, calcium nitrate solution was prepared by treating WMP with the nitric acid solution. It was further treated with potassium dihydrogen phosphate (KH_2PO_4) and ammonia solution (NH_4OH) to synthesize hydroxyapatite (MA-Hap LR 72) powder. Four hundred ninety millilitre of 0.32 M calcium nitrate solution was prepared from WMP, which was treated with 0.19 M KH_2PO_4 solution (930 g by wt.) and 1 M NH_4OH solution (1000 mL). The formation of pure Hap free of other calcium phosphate impurities was ensured by maintaining a Ca:P molar ratio of 1.67 in the reaction mixture. The pH of the solution was maintained at 9 pH by adding NH_4OH. The solution was stirred using a stirrer (600 to 1000 rpm), and the reaction mixture was maintained at a temperature of 72 °C. A white gel-like Hap precipitated, which was aged overnight, centrifuged, washed with distilled water, and dried under controlled conditions at 110 °C to obtain hydroxyapatite powder. The yield of MA-Hap LR 72 powder per batch while using a batch reactor of 60L capacity was 470 g. The MA-Hap LR 72 powder prepared had a rod-shaped morphology with a specific surface area of 24.66m^2/g, while the pore volume was observed to be 0.096 cm^3/g (George et al. 2022). The Hap powder was mixed with 10 g of PVA and 1.05 g of malonic acid, which served as binders to form Hap paste. The paste was transformed into pellets by the extrusion spheronization technique as described in Fig. 1. The gel was aged overnight, centrifuged, washed, and dried at 110 °C under controlled conditions to obtain hydroxyapatite powder. The MA-Hap LR 72 powder prepared had a rod-shaped morphology with a surface area of 24.66m^2/g (George et al. 2022) determined using a BET surface area analyser (Quantachrome, Autosorb-1). The powder was transformed into pellets by the extrusion spheronization techniques using a binder of polyvinyl alcohol as

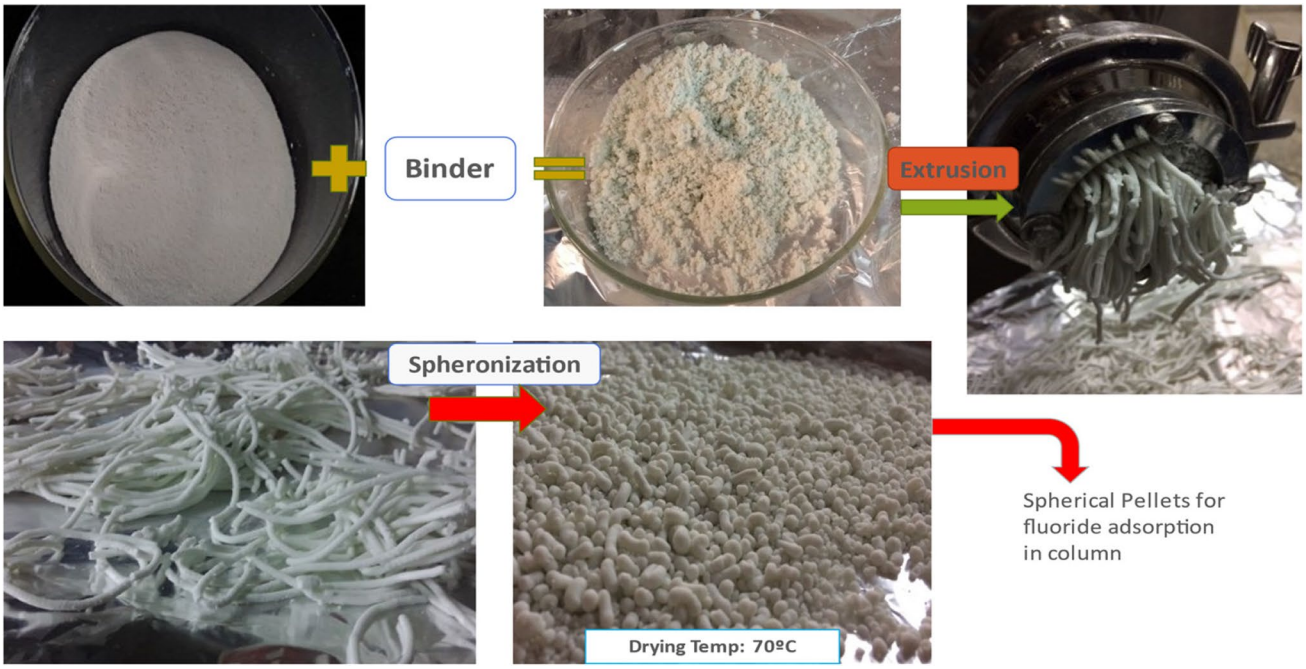

Fig. 1 Preparation of MA-Hap LR pellets for adsorption

described in Fig. 1. Spherical pellets of size 2–3 mm were produced using a spheronizer with a spherical multi-hole plate rotating at around 800 rpm. These MA-Hap LR pellets were dried at 75 °C for 4 h and used in an adsorption column for fluoride removal experiments.

The fluoride removal capacity of MA-Hap LR was estimated by treating specific dosages of the adsorbent with 10 mg/L of fluoride samples. The treated solution was filtered, and the filtrate was analysed for residual fluoride concentrations using an ion-selective electrode (Thermo Scientific Orion Versa 5 star). For fluoride analysis, a fluoride stock solution of 1000 mg/L was prepared using analytical grade sodium fluoride (2.21 g NaF in 1 L of double distilled water), and a working solution of 10 mg/L concentration was obtained by appropriate dilution from the stock solution. The instrument was calibrated using fluoride standards of concentrations varying from 0.1 to 10 mg/L. To avoid ionic interference, an ionic strength buffer TISAB-II was added to the fluoride samples in a ratio of 1:1. The total ionic strength adjustment buffer (TISAB-II) was prepared by taking 58 g of NaCl, 4 g of CDTA, and 57 mL of glacial acetic acid. For adjusting the pH of the buffer to 5.5, 5 M NaOH solution was used. Water quality parameters such as TDS, electrical conductivity, and amount of calcium leached into treated water during adsorption were determined using an ion analyser. The hardness, alkalinity, and concentration of magnesium and phosphorus in the solution were analysed using standard APHA methodologies (APHA/AWWA/WEF 2012).

Column breakthrough performances for fluoride adsorption

Continuous column experimental studies were carried out at room temperature using an adsorption column setup, as shown in Fig. 2. A column of 50 cm in length and 5.0 cm in diameter was used to evaluate the column fluoride adsorption capacity of MA-Hap LR 72 pellets. The column was packed with MA-Hap LR 72 pellets, and feed fluoride solution was pumped across the packed bed with a magnetic drive pump from a stainless steel tank of 20 L capacity at a controlled inlet feed flow rate. The effect of various process parameters such as bed height, inlet flow rate, initial fluoride concentration, and particle size of pellets on adsorption breakthrough curves (BTC) was studied. Samples were collected from the column outlet and analysed at regular intervals. The effect of bed height on fluoride removal capacity was studied for three different bed heights, i.e. 5, 10, and 15 cm bed height, for treating the influent fluoride concentration of 10 mg/L and flow rate at 1 LPH. The effect of flow rate on fluoride removal was studied at different flow rates of 1, 1.5, and 2 LPH, using 104 g (25 cm bed height) of adsorbent for treating fluoride concentration of 10 mg/L. The effect of the initial fluoride concentration of the column feed was studied for varying concentrations, i.e. 5, 10, and 15 mg/L, when passed through the column packed with 104 g (25 cm) of MA-Hap LR 72 pellets at a constant flow rate of 1 LPH. The BTC curves acquired were plotted in terms of the ratio of

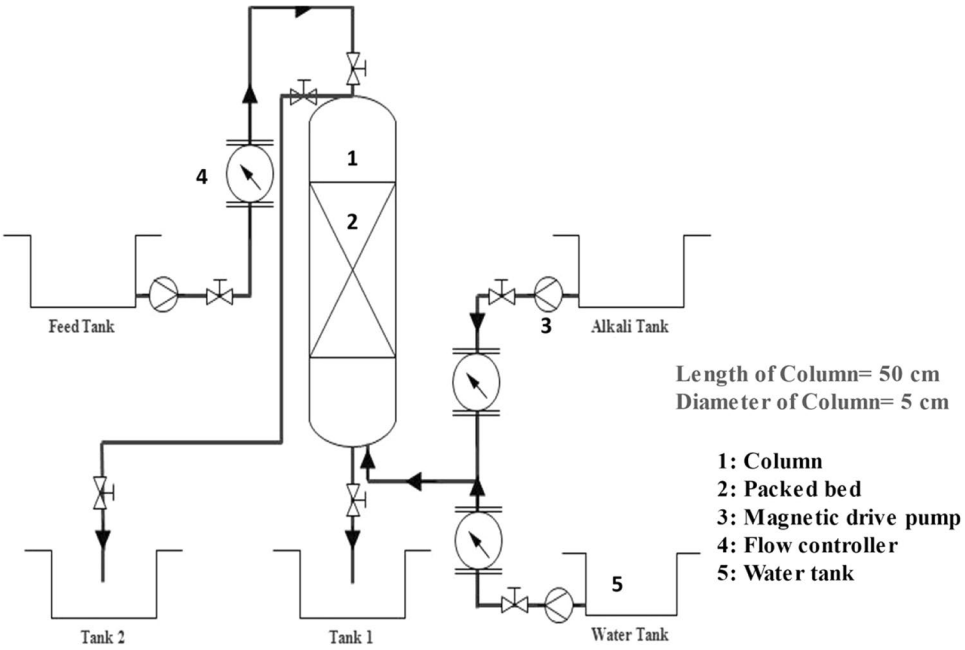

Fig. 2 Experimental setup for fluoride adsorption studies on MA-Hap LR pellets

outlet fluoride concentration to inlet fluoride concentration to time, i.e. C_e/C_0 vs time. The breakthrough capacity (q_b) is defined as the total quantity of fluoride ions adsorbed by MA-Hap LR 72 pellets when the fluoride concentration in the column effluent reaches ≈5% of the initial concentration. The q_b (mg/g) can be estimated from the area under the breakthrough curve for a known fluoride concentration according to Eq. 1. C_0 and C_t are the inlet and outlet fluoride concentrations, respectively (mg/L); M is the mass of adsorbent (g), and t_b is the time (L) at the breakthrough point. The breakthrough point was considered at a residual fluoride concentration of 1.0 mg/L (the permissible limit for fluoride in the water). The capacity at the exhaustion point (q_{EX}) corresponds to the quantity of fluoride adsorbed by MA-Hap LR 72 pellets when the fluoride outlet concentration reaches approximately 95% of the initial value. It is estimated using Eq. 2, where q_{EX} is the capacity at the exhaustion point (mg/g) and t_{EX} is the exhaustion time when the column is saturated (h). The empty bed contact time (EBCT) is estimated using Eq. 3, where Z is bed height in cm and F is the volumetric flow rate L/h.

$$q_b = \int_0^{t_b} \frac{C_o - C_t}{M} dt \tag{1}$$

$$q_{EX} = \int_0^{t_{EX}} \frac{C_o - C_t}{M} dt \tag{2}$$

$$EBCT = \frac{Z}{F} \tag{3}$$

Modelling of breakthrough profile in column studies

Models help represent and predict the fluoride adsorption breakthrough behaviour with high accuracy, efficiency, and applicability from lab-scale experiments. Two column breakthrough models, viz. Thomas model and Yoon–Nelson model, were used to fit the experimental data obtained from the column performance for removing fluoride from aqueous solution using MA-Hap LR 72 pellets. The Thomas model represents the adsorption behaviour in fixed-bed columns, which is defined according to Eq. 4. Here, K_{th} (L/mg h) is the Thomas rate constant, q_0 (mg/g) is the equilibrium adsorbate uptake, and M is the mass of MA-Hap LR pellets in the column. The model assumption is that process follows Langmuir kinetics of adsorption–desorption with no axial dispersion. Thomas's model derivation is based on second-order kinetics, and it considers that adsorption is not affected by the chemical reaction but by the mass transfer at the interface (Bharathi and Ramesh 2013).

Yoon–Nelson model Yoon and Nelson developed a less complex model as information related to characteristics of adsorbate, adsorbent type, and the physical properties of the adsorption bed is not used. The assumption in Yoon and Nelson model is that the rate of decrease in the probability of adsorption of an adsorbate molecule is proportional to the probability of the adsorbate adsorption and the probability of an adsorbate breakthrough on the adsorbent (Yoon and Nelson 1984). The linearized form of the Yoon–Nelson equation is given in Eq. 5, where k_γ (h^{-1}) is the Yoon–Nelson rate

constant and τ (h) is the time required for 50% adsorbate breakthrough time:

$$\ln\left(\frac{C_0}{C_b}-1\right)=K_{th}q_0\frac{M}{F}-K_{th}C_0t \tag{4}$$

$$\ln\left(\frac{C_e}{C_0-C_e}\right)=k_\gamma t-\tau k_\gamma \tag{5}$$

Column design parameters

The experimental breakthrough curves were studied for the estimation of column design parameters, such as t_x (time to establish primary adsorption zone), t_f (time for the formation of primary adsorption zone), t_z (time for movement of primary adsorption zone down the column), δ (length of primary adsorption zone), f (fractional capacity of pellets in adsorption zone), $\%S$ (percentage saturation in the column), and H_{UNB} (unused bed height). The primary adsorption zone (PAZ) is the part of the adsorbent bed present between exhaustion concentration (C_{EX}) and the concentration for breakthrough (C_b). The time to establish the primary adsorption zone (t_x) is the time needed for the primary adsorption zone to establish and move out of the adsorption column. It is defined by Eq. 6. The time required for the movement of PAZ down the column (t_z) is calculated by Eq. 7. For a bed depth Z for pellets, the depth and time ratios are computed from Eq. 8 (Ghosh et al. 2015). The time for the formation of PAZ (t_f) is estimated using Eq. 9. The fractional capacity (f) and percentage saturation of the adsorption column ($\%S$) is estimated by Eq. 10 and Eq. 11, respectively. The height of the unused bed (H_{UNB}) in the adsorption column is estimated using Eq. 12. The number of bed volumes (B.V.) treated before the breakthrough point and the adsorbent exhaustion rate (AER) indicates the performance of the column. The greater the number of bed volumes before the breakthrough point, the better the performance of the adsorption column system. The adsorption exhaustion rate is determined from the mass of adsorbent used per unit volume of solution treated at a breakpoint (AER), representing the goodness of the adsorbent bed performance:

$$t_x=\frac{V_{EX}}{F} \tag{6}$$

$$t_z=\frac{V_{EX}-V_b}{F} \tag{7}$$

$$\frac{\delta}{Z}=\frac{t_z}{t_x-t_f} \tag{8}$$

$$t_f=(1-f)\delta \tag{9}$$

$$f=\frac{\int_{V_b}^{V_{EX}}(C_0-C_t)dv}{C_0(V_{EX}-V_B)} \tag{10}$$

$$\%S=\left[1+\frac{\delta(f-1)}{Z}\right]X100 \tag{11}$$

$$H_{UNB}=\frac{Z}{t_{EX}}(t_{EX}-t_b) \tag{12}$$

Results and discussion

Breakthrough performances for fluoride adsorption by MA-HAP LR 72 pellets

The column breakthrough curves were studied to determine the effect of varying pellet sizes, influent flow rates, bed depth, and initial fluoride concentrations on the fluoride adsorption capacity, which is depicted in Fig. 3. The various breakthrough curve parameters for variations in particle size, varying bed heights, varying flow rates, and varying inlet feed concentrations are also presented in Table 1. Variation of the inlet feed flow rate into the column significantly affects the column performance, and the optimum flow rate needs to be identified for the best column fluid flow dynamics (Saha et al. 2012). By varying the feed flow rates at 1, 1.5, and 2 LPH (i.e. 16, 25, and 33 mL/min) for a constant bed height of 25 cm and inlet fluoride concentration at 10 mg/L, the effect of flow rate on fluoride adsorption capacity of MA-Hap LR 72 pellets was examined. The BTC curves are shown in Fig. 3a. The breakthrough time and adsorption capacity decreased with the increase in flow rate. As the flow rate increased, the mass transfer zone quickly moved out of the column, and the residence time of fluoride ions in the column decreased, which lowered the adsorption capacity. At lower flow rates, fluoride ions have more contact time with the MA-Hap LR 72 pellets, resulting in a narrower mass transfer adsorption zone which causes higher adsorption capacity. The treated volume up to breakpoint was 14 L, 10.5 L, and 8 L for 1 LPH, 1.5 LPH, and 2 LPH, respectively. The empty bed contact time (EBCT), a critical parameter determining the residence time between the adsorbent and the adsorbate, was observed to be 29.4 min, 19.6 min, and 14.7 min for the flow rates of 1 LPH, 1.5 LPH, and 2 LPH respectively. A decrease in flow rate causes an increase in EBCT; hence, fluoride ions get more time to contact the adsorbent, resulting in higher column defluoridation capacity.

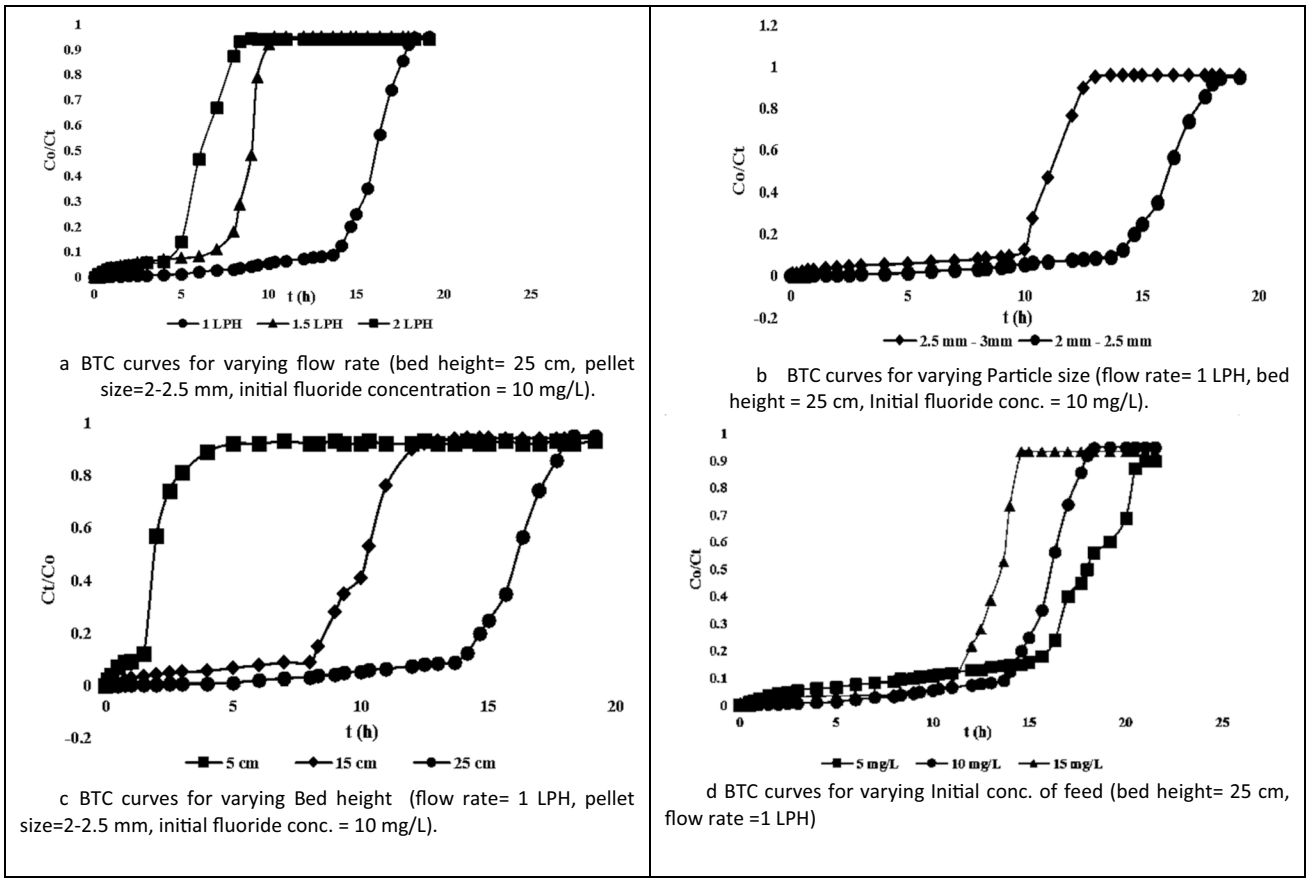

a BTC curves for varying flow rate (bed height= 25 cm, pellet size=2-2.5 mm, initial fluoride concentration = 10 mg/L).

b BTC curves for varying Particle size (flow rate= 1 LPH, bed height = 25 cm, Initial fluoride conc. = 10 mg/L).

c BTC curves for varying Bed height (flow rate= 1 LPH, pellet size=2-2.5 mm, initial fluoride conc. = 10 mg/L).

d BTC curves for varying Initial conc. of feed (bed height= 25 cm, flow rate =1 LPH)

Fig. 3 Effect of varying parameters on the column breakthrough curves (BTC)

Table 1 Breakthrough parameters by MA-Hap LR 72 pellets

Parameters	q_b (mg/g)	q_{EX} (mg/g)	t_b (h)	t_{EX} (h)	V_b (L)	V_{EX} (L)
Particle size (mm)						
2–2.5	1.21	1.55	14	18	14	18
2.5–3	0.865	1.04	10	12	10	12
Bed height (cm)						
5	0.64	1.71	1.5	4	1.5	4
15	1.1	1.6	8	11	8	11
25	1.21	1.55	14	18	14	18
Flow rate (LPH)						
1	1.21	1.55	14	18	14	18
1.5	1.038	1.29	7	10	10.5	15
2	0.692	1.03	4	6	8	12
Initial fluoride (mg/L)						
5	0.692	0.78	16	21	16	21
10	1.21	1.55	14	18	14	18
15	1.615	2.01	12	15	12	15

The BTC curves were obtained for varying pellet sizes, i.e. for two different particle sizes, 2–2.5 mm and 2.5–3 mm, while keeping flow rate at 1 LPH, bed height at 25 cm, and inlet fluoride concentration at 10 mg/L is shown in Fig. 3b. With the increase in particle size from 2.0–2.5 mm to 2.5–3 mm, breakthrough time decreases considerably, and breakthrough adsorption capacity decreases from 1.21 to 0.865 mg/g because smaller

particles have a higher surface area, causing higher adsorption capacity.

The effect of bed height on BTC was determined by passing a fluoride solution of concentration 10 mg/L at the flow rate of 1 LPH through different bed heights, i.e. 5 cm, 15 cm, and 25 cm, and breakthrough time increased from 1.5 to 14 h with an increase in bed height from 5 to 25 cm as depicted in Fig. 3c. The residence time of fluoridated solution inside the column increased with increased bed heights as the mass transfer zone moved slowly down the column, allowing higher contact time and fluoride removal efficiency. The corresponding breakthrough capacities are 0.64 mg/g, 1.1 mg/g, and 1.21 mg/g, while the volume of solution treated up to the breakthrough point is 1.5 L, 8 L, and 14 L for 5 cm, 15 cm, and 25 cm bed heights, respectively. A bed height of 25 cm has a higher adsorption capacity than other bed heights.

The adsorbent has a specific adsorption capacity; therefore, the breakthrough profile depends on the influent fluoride concentration. The breakthrough curves for the inlet adsorbate concentrations of 5, 10, and 15 mg/L are shown in Fig. 3d. As fluoride concentration increased from 5 mg/L, 10 mg/L, and to 15 mg/L, the breakthrough time was 16 h, 14 h, and 12 h, whereas the exhaustion time was 21 h, 18 h, and 15 h, respectively. The treated volume up to the breakthrough point was 16 L, 14 L, and 12 L, respectively. With an increase in fluoride concentration, fast saturation occurred, i.e. sorption sites of the adsorbent got exhausted, leading to the earlier breakthrough. The binding sites of the bed saturated more quickly, leading to earlier breakthroughs and shorter exhaustion time. The adsorption capacity of MA-Hap LR 72 pellets at the breakpoint and exhaustion point was observed to increase from 0.692 to 1.615 mg/g and 0.78 to 2.01 mg/g, respectively, with an increase in fluoride concentration from 5 to 15 mg/L. However, the breakthrough corresponded to a relatively wide mass transfer zone (MTZ) for low fluoride concentration. The delayed BTCs for lower fluoride concentration indicate that the volume treated will be higher since the lower concentration gradient caused slower transport due to decreased diffusion coefficient. It has been observed that for efficient column performance, smaller particle size, greater bed height, and slow flow rate are required. With the increase in feed concentration, the adsorption capacity was increased, but the column saturation was faster, and the breakthrough time was decreased.

The design parameters were estimated for efficient column performances and listed in Table 2. It can be observed that the time required for forming the primary adsorption zone (PAZ) reduced with a decrease in adsorbent bed height, rise in inflow rate of fluoridated water, and initial fluoride concentration. That means the more the bed height, the more time it takes to form the PAZ. Likewise, with the reduction in flow rate, the contact time required to form the adsorption zone also decreases. The length of the adsorption zone increases as the bed height and flow rate increase. On the other hand, the percentage saturation for the adsorption column increased with bed height and decreased as the flow rate increased. However, the fractional capacity of the column at the breakthrough point declined with an increase in flow rate, initial fluoride concentration, and increasing adsorbent bed height. The fractional capacity of MA-Hap LR 72 pellets in the adsorption zone decreased, attributing to a smaller number of F- ions available per active site with an increase in the bed height of the adsorbent. When the flow rate increased, the adsorption zone's length also increased, while the percentage saturation decreased as the adsorption zone travelled quicker.

Additionally, due to the greater degree of freedom of the F- ions over the MA-Hap LR 72 adsorbent pellet surface, the adsorption zone was found to reduce with an increase in the initial fluoride concentration of the feed water. Table 3 shows that when a higher bed height of adsorbent was used, the adsorbent bed remained unused. Similarly, the unused adsorbent bed height was also high when the flow rate was higher.

The values of bed volumes (B.V.) processed and adsorbent exhaustion rate (AER) are presented are given in Table 3. It was observed that the number of processed B.V.s before the breakthrough increased with the bed height, while it decreased with an increase in flow rate, initial fluoride concentration, and particle size. As predicted, the AER was faster at elevated flow rates, lower bed heights, larger particle sizes, and higher fluoride concentrations. Many

Table 2 Column design parameters

	Z (cm)			F (L/h)			C_0 (mg/L)		
Parameters	5	15	25	1	1.5	2	5	10	15
t_x (h)	4	11	18	18	10	6	21	18	15
t_z (h)	2.5	3	4	4	3	2	5	4	3
t_f (h)	1.37	1.65	2.13	2.13	1.8	1.25	2.5	2.13	1.74
δ (cm)	4.77	4.81	6.3	6.3	9.14	10.52	6.75	6.3	5.65
F	0.45	0.45	0.466	0.466	0.4	0.375	0.5	0.466	0.42
%S	47.53	82.3	86.5	86.5	78	73.5	86.5	86.5	86.8
H_{UNB}	3.12	4.1	5.48	5.48	7.4	8.2	5.87	5.48	4.91

Table 3 Column performance indicators at various operating conditions

Parameter	Z (cm)			F (L/h)			C_0 (mg/L)			Particle size (mm)	
	5	15	25	1	1.5	2	5	10	15	2–2.5	2.5–3
B.V.s processed	15.29	27.1	28.5	28.5	14.28	8.16	32.65	28.5	24.4	28.5	20.4
AER (g/L)	14	7.8	7.4	7.4	14.8	26	6.5	7.4	8.6	7.4	10.4

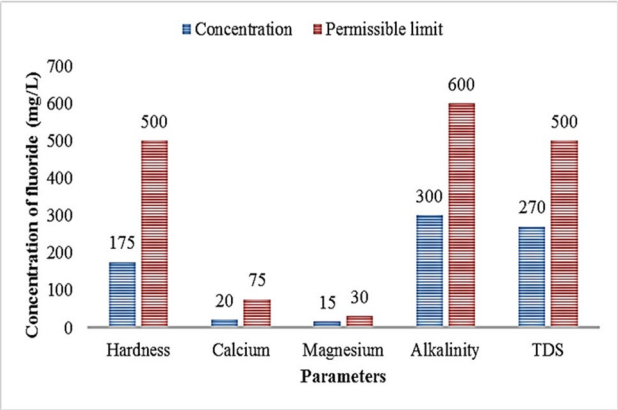

Fig. 4 Treated water quality using Ma-Hap LR 72 pellets

other researchers have reported the same trend of B.V. and AER(Malkoc et al. 2006; Baral et al. 2009; Ghosh et al. 2015). The optimum conditions derived from the breakthrough profiles indicate that a bed height of 25 cm with a flow rate of 1 LPH and feed concentration 10 mg/L was found optimum for efficient column performance with maximum percentage saturation of the bed.

Treated water quality parameters

The water quality treated with MA-Hap LR 72 pellets determines its feasibility for practical applications. As observed in the breakthrough profiles, the breakthrough fluoride concentration in treated water is below 1 mg/L, which is the permissible limit of fluoride in drinking water. The other parameters studied include hardness, calcium, magnesium, alkalinity, and TDS, and their values obtained are shown in Fig. 4. The hardness of treated water was 175 mg/L, whereas calcium and magnesium concentrations were 20 mg/L and 15 mg/L, respectively, which are within permissible limits. The treated water's pH was 7.43, which is an acceptable drinking water pH. The value of alkalinity and TDS was also under the permissible limit making the treated water suitable for drinking purposes. Thus, the adsorbent MA-Hap LR 72 pellets have the potential to treat high fluoride concentrated (10 mg/L) water to concentrations below 1 mg/L with a column capacity of around 1.615 mg/g, which makes it suitable for practical applications.

Modelling of adsorption kinetics

Two mathematical models were studied to represent the adsorption behaviour of fluoride ions in the column packed with MA-Hap LR 72 pellets, viz. Thomas model and the Yoon–Nelson model.

Thomas model Thomas model was applied to the adsorption kinetic data for three different bed heights, flow rates, feed concentrations, and particle sizes. The Thomas rate constant (K_{th}) and the Thomas adsorption capacity (q_0) were calculated from the slope and intercept of the plot between ln (C_0/C_e-1) versus t (h), as shown in Fig. 5a–d.

The calculated values of K_{th} and q_0, along with the regression coefficients (R^2), are presented in Table 4.

The comparatively higher value of R^2 at all the operating conditions suggested that the Thomas model was suitable for describing the column adsorption data of fluoride by MA-Hap LR 72. It was observed that the value of K_{th}' decreased with an increase in bed depth, flow rate, and initial fluoride concentrations. This may be due to increased mass transport resistance as it is proportional to axial dispersion and thickness of the liquid film on the particle surface (Malkoc et al. 2006). With the increase in bed height, the value of q_0 increased because of the greater contact time of fluoride ions with MA-Hap pellets. With the increase in flow rate, the value of K_{th} was increased, whereas the value of q_0 decreased because of faster exhaustion of adsorbent and lesser mass transport resistance. The value of q_0 was higher, i.e. 4.2 mg/L at a higher fluoride concentration. More fluoride ions were loaded per unit active site of adsorbent, which causes faster saturation and lower throughput volume. In the case of particle size, the value of q_0 decreased from 1.66 to 0.686 mg/g, while the value of K_{th} increased. This can be because adsorbents with smaller particle sizes have a large surface area for adsorption, and hence, Thomas's adsorption capacity was high.

Yoon–Nelson model Yoon–Nelson model was also applied to the column experimental data for fluoride adsorption by MA-Hap LR 72 pellets. The values of k_Y (Yoon–Nelson rate constant) and τ (time required for 50% adsorbate breakthrough) were determined from the graph between ln (C_e/C_0-C_e) vs t at varying flow rates, bed heights, particle sizes, and feed fluoride concentrations as shown in Fig. 6a–d. The

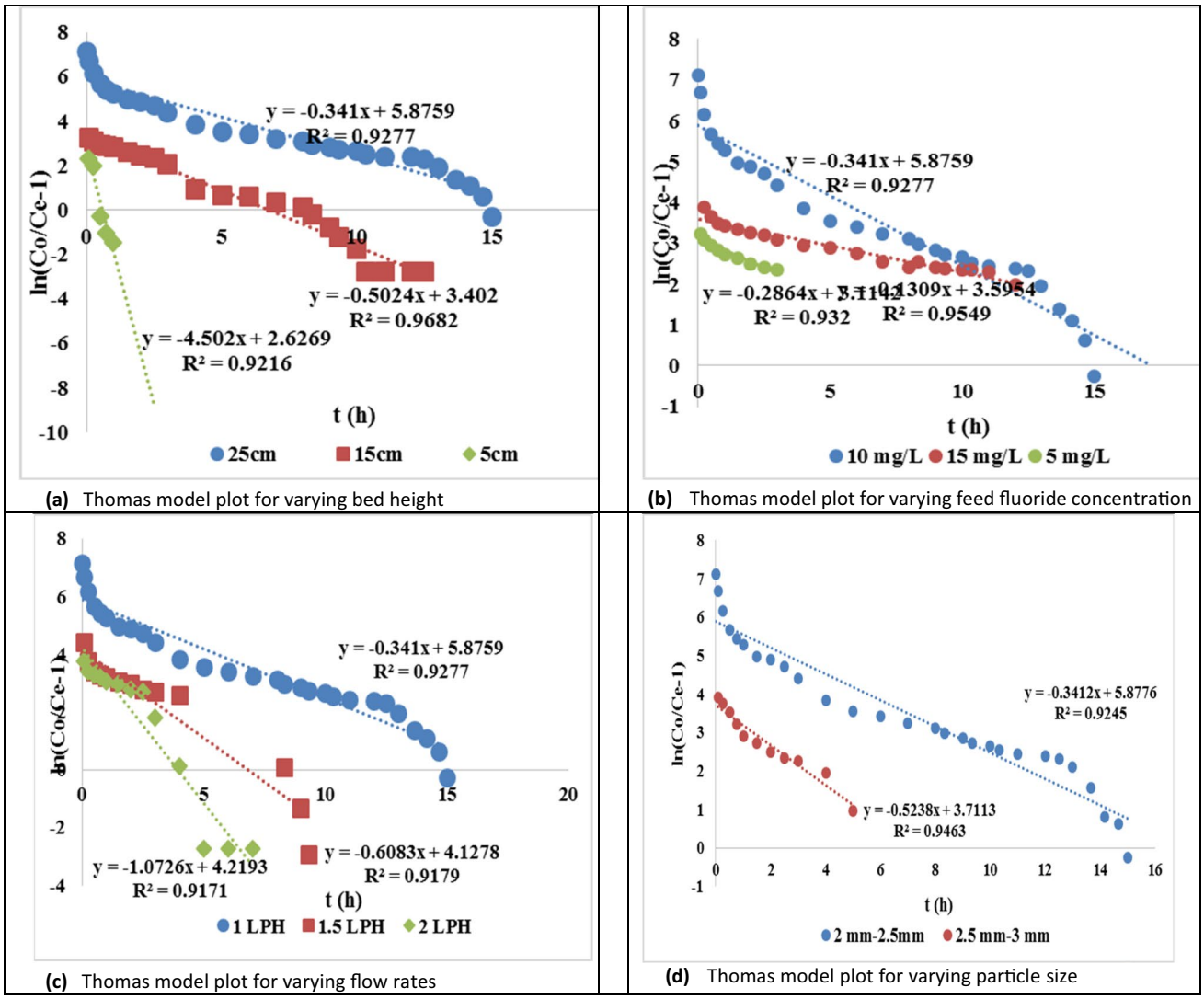

Fig. 5 **a** Thomas model plot for varying bed height. **b** Thomas model plot for varying feed fluoride concentration. **c** Thomas model plot for varying flow rates. **d** Thomas model plot for varying particle size

Table 4 Kinetic parameters for the Thomas model

	Bed height (cm)			Flow rate (LPH)			Initial F (mg/L)			Particle size (mm)	
Parameters	25	15	5	1	1.5	2	5	10	15	2–2.5	2.5–3
K_{th} (L/mg h)	0.034	0.050	0.45	0.034	0.060	0.1	0.057	0.034	0.008	0.034	0.052
q_0 (mg/g)	1.66	1.07	0.277	1.66	0.99	0.8	0.525	1.66	4.2	1.66	0.686
R^2	0.927	0.968	0.921	0.927	0.917	0.917	0.932	0.927	0.955	0.927	0.946

values of different Yoon–Nelson parameters are also given in Table 5. The values of τ' increase with the increase in bed height, whereas it decreases with an increase in flow rate, fluoride concentration, and particle size. Moreover, the correlation coefficient (R^2) value was less than 0.96 for most of the parameters, showing poor fitting compared to the Thomas model.

Regeneration of MA-HAP LR 72 adsorbent

The regeneration and reutilizing of the adsorbent are significant aspects of cost-effective adsorption technology. The optimal concentration of regenerant/eluent solution is also crucial as it can adversely affect adsorbent characteristics. The exhausted adsorbent was regenerated using different

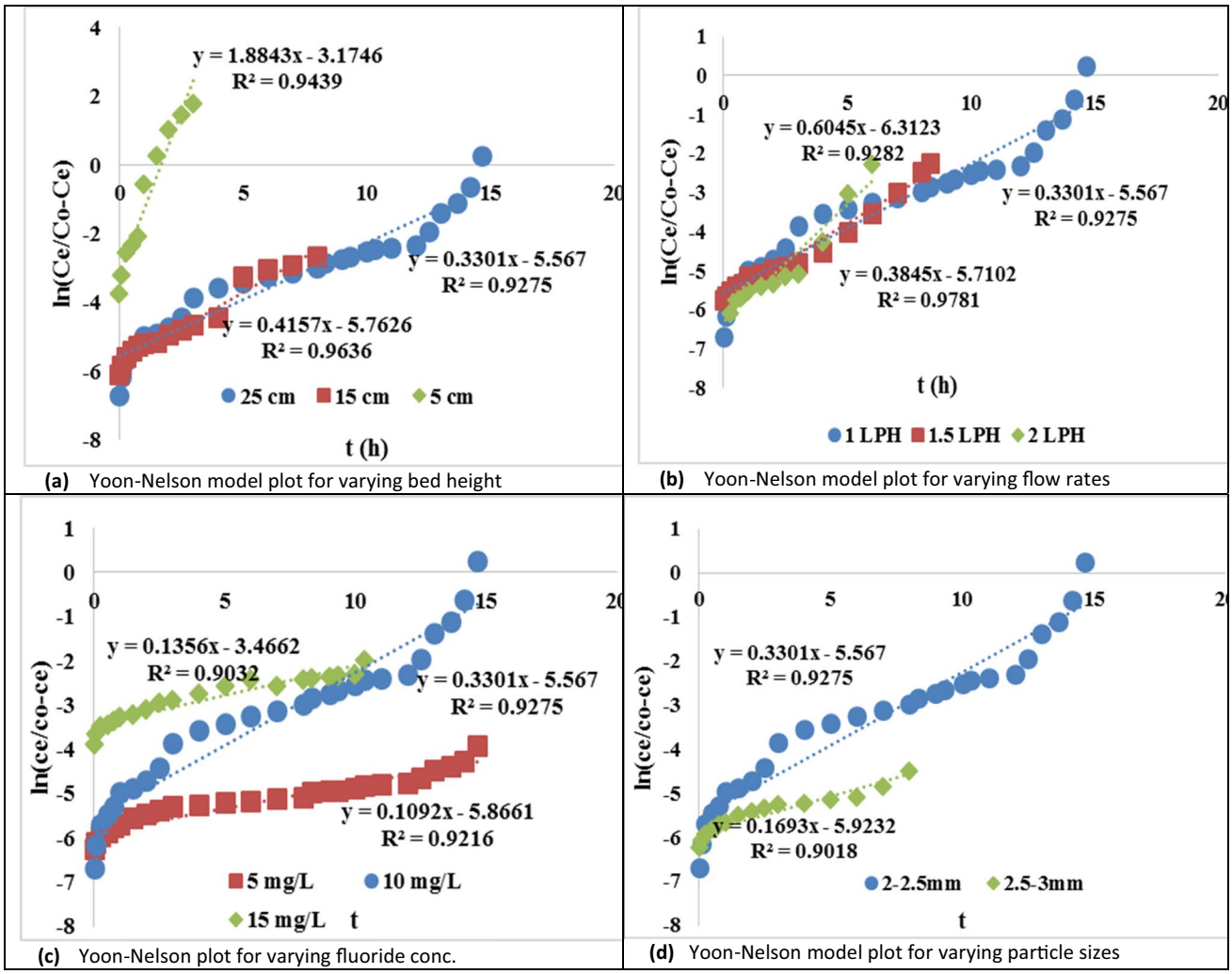

Fig. 6 **a** Yoon–Nelson model plot for varying bed height. **b** Yoon–Nelson model plot for varying flow rates. **c** Yoon–Nelson plot for varying fluoride concentrations. **d** Yoon–Nelson model plot for varying particle sizes

Table 5 Kinetic parameters for the Yoon–Nelson model

Parameter	Z (cm)			F (L/h)			C_0 (mg/L)			Particle size (mm)	
	5	15	25	1	1.5	2	5	10	15	2–2.5	2.5–3
k_Y (h^{-1})	1.88	0.415	0.331	0.331	0.384	0.604	0.109	0.331	0.169	0.331	0.169
τ (h)	1.688	13.88	16.81	16.81	14.85	10.45	53.81	16.81	3.49	16.81	0.349
R^2	0.943	0.963	0.927	0.927	0.973	0.928	0.921	0.927	0.901	0.927	0.901

concentrations of eluent (NaOH) ranging from 0.1 to 1.5 M. The up-flow mode of the eluent was used at a flow rate of 1 LPH for faster regeneration and to cause better contact between the exhausted bed and the eluent. Regeneration of saturated pellets was done with different concentrations of NaOH varying from 0.1 to 1.5 M.

Figure 7 depicts the XRD spectra of MA-Hap LR 72 pellets in their unsaturated (a), exhausted (b), and regenerated forms (c–f) at different regenerant concentrations (0.1 M, 0.5 M, 1 M and 1.5 M). The spectra obtained from exhausted MA-Hap LR 72 pellets depict fluorapatite formation. A comparison of spectra of fresh and exhausted pellets indicates that the OH^- ions of hydroxyapatite have been replaced with F- ions due to the formation of fluorapatite. When different concentrations of NaOH were used for regeneration, it was observed from Fig. 7c–e that the extent of regeneration

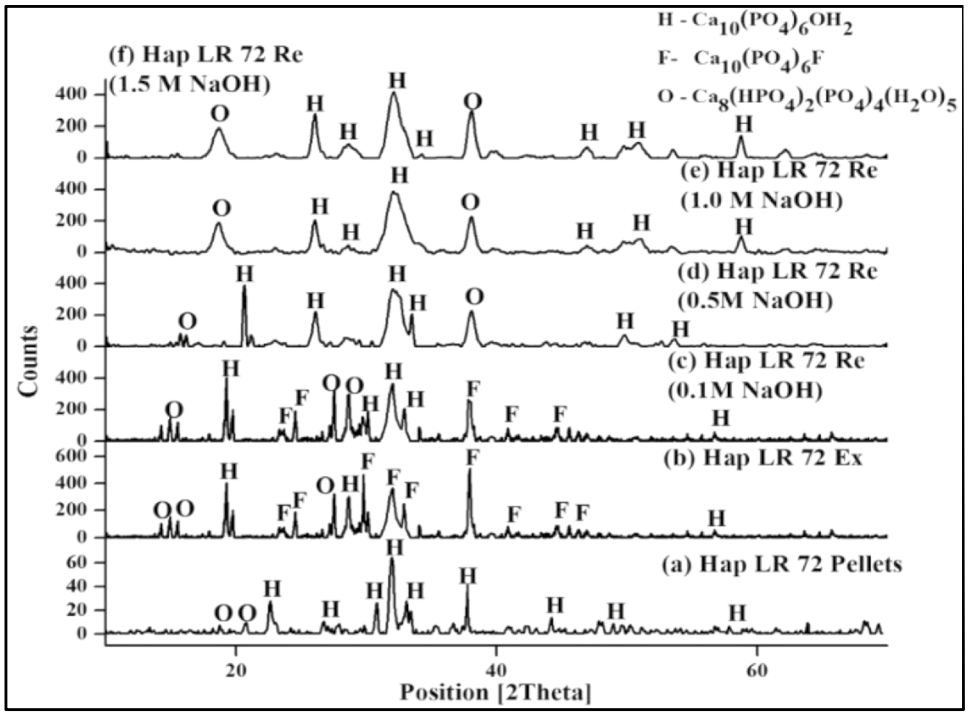

Fig. 7 XRD spectra of MA-Hap LR 72 pellets: (**a**) unsaturated, **b** exhausted, **c** regenerated at 0.1 M, **d** regenerated at 0.5 M, **e** regenerated at 1.0 M, **f** regenerated at 1.5 M

increased with the increase in eluent concentration. There was no significant difference between the XRD spectra of 1.0 M and 1.5 M NaOH concentration; therefore, 1.0 M NaOH was optimum for regenerating MA-Hap LR 72 pellets.

The adsorbent bed was later washed with distilled water for approximately 4 h at the same flow rate until the pH of the outlet solution was neutral (7.0 ± 0.2). After that, the reactivated MA-Hap LR 72 pellets were ready for the next defluoridation cycle. Altogether, four cycles of regeneration experiments were conducted, and the fluoride adsorption capacities for the four cycles are depicted in Fig. 8. The fourth cycle's capacity was very low, indicating that the adsorbent could be effectively used for three cycles.

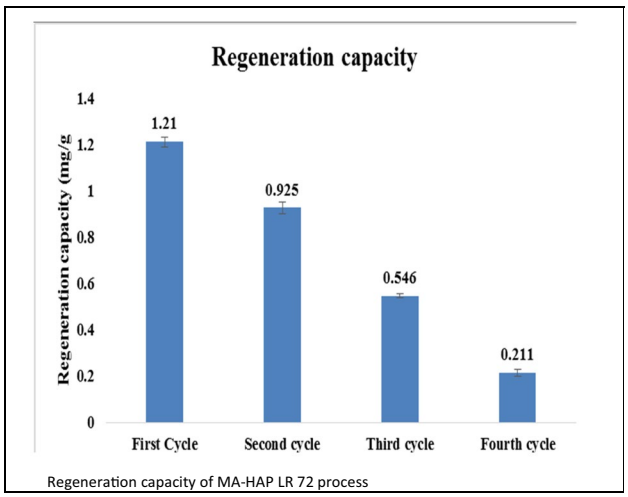

Fig. 8 Regeneration capacity of MA-HAP LR 72 pellets

Community-level plant for treating 10KL per day using MA-Hap LR 72 pellets for fluoride water of 10 mg/L concentration

The experimental breakthrough curves and column performance indicators in Table 5 indicate that a maximum bed height of 25 cm with an inlet flow rate of 1 LPH for a feed concentration of 10 mg/L was optimum for efficient column performance. The breakthrough column performance was at a maximum adsorption capacity of 1.21 mg/g, treating 10 mg/L fluoride concentration/-. The optimized column flow rate at 1 LPH using an adsorbent bed height of 25 cm processed 28.5-bed volumes at an adsorbent exhaustion rate of 7.4 g/L. Based on these optimized column parameters, the calculations were carried out to design a community-level defluoridation plant to treat 10,000 L/day, and the details are given in the Appendix. The column design parameters are summarized in the following Table 6.

The cost involved in synthesizing per kilogramme of MA-Hap LR pellets is Rs. 1.0188/g on a pilot plant scale of 60L capacity (George et al. 2022). In designing the MA-Hap LR adsorber column for treating 10,000 L of fluoride water (10 mg/L concentration) a day, the column parameters are a bed height of 0.24 m and a column diameter of 0.799 m. The bed volume contained 199.2 kg of MA-HAP pellets, and the adsorbent pellets cost Rs. 202,945/-. The maximum

Table 6 MA-Hap adsorbent column parameters

Adsorbent	Density (kg/m^3)	Avg. pellet size (mm)	Bed height (cm)	Flow rate (LPH)	Initial fluoride concentration (mg/L)	Diameter (D_p) m	Filtration rate (F.R.) m/min	New bed height (h_p) m	Mass of adsorbent (kg)
MA-Hap LR	1660	2–2.5	25	1	10	0.799	0.0138	0.24	199.2

bed adsorption capacity is at 1.21 mg/g, and the adsorbent exhaustion rate at column breakthrough is 7.4 g/L. Therefore, the bed of 199.2 kg will treat 26,918 L of fluoride water at column breakthrough. Hence, the fluoride treatment cost of 10 mg/L concentrated fluoride water by the MA-Hap LR pellets within the adsorption column is estimated at Rs 7.53 per litre, which can be slightly higher after including the operating cost (pumping costs involved) of the treatment plant.

Conclusions

Marble hydroxyapatite pellets prepared from waste marble slurry are suitable adsorbents for fluoride water treatment. The column studies were carried out to identify optimum column operational parameters like flow rate, initial fluoride concentration, particle size, and bed height for optimum operating conditions. The column adsorption capacity for MA-HAP LR 72 pellets was 1.21 mg/g for treating fluoride concentration of 10 mg/L at 1 LPH flow rate and a bed height of 25 cm, which processed 28.5-bed volumes at an AER of 7.4 g/L. Thomas's model fitted well for the column breakthrough performance data with a high correlation coefficient value. Regeneration of the MA-Hap LR 72 pellets could be done for up to three cycles using a 1.0 M NaOH solution. Assessment of treated water quality for pH, alkalinity, hardness, and TDS using MA-HAP pellets suggested acceptable according to WHO and BIS regulations. Marble slurry waste powder, otherwise considered waste, is actually a useful resource for making environment-friendly and cheap hydroxyapatite adsorbent that can alleviate the problem of fluorosis by providing fluoride-free clean drinking water.

Appendix

Adsorber column calculations.
Height of packed column = 25 cm = 0.25 m.
Column diameter (d) = 4 cm = 0.04 m.
Q = inlet flow rate = 1 LPH = 16.66 mL/min = 1.66×10^{-5} m^3/min.
Density of Ma-Hap = 1660 kg/$m.^3$
Column cross-sectional area (A) = $\frac{\pi}{4}d^2 = 1.2 \times 10^{-3}$ $m.^2$
Filtration rate (FR) = Q/A = 1.38×10^{-2} m/min.
For a unit of 10,000 L/day (6.94×10^{-3} m^3/min) the required height and diameter of the column would be.
Area of the new column = Q/FR = $6.94 \times 10^{-3}/1.38 \times 10^{-2} = 5.02 \times 10^{-1}$ $m.^2$
New diameter (D_p) of column = 0.799 m.
Bed volume (AxH) = $0.25 \times 1.2 \times 10^{-3} = 0.3$ $m^3 = 300$ mL.
Bed contact time = V/Q = 300/16.66 = 18.00 min.
New bed height (h_p) = $18.00 \times 0.0138 = 0.24$ m.
Volume of column (V_p) = $\frac{\pi}{4}D_p{}^2 h_p$ = 0.120 $m.^3$
Mass of adsorbent required to treat 10,000 L = volume × density = $0.120 \times 1660 = 199.2$ kg.
Adsorbent exhaustion rate at column breakthrough is 7.4 g/L.
Amount of fluoride water that can be treated = 199,200/7.4 = 26,918 L.
Treatment cost per litre of water = Rs. 202,945/26,918 = Rs. 7.53.

Author contribution Dhiraj Mehta: conceptualization, data curation, writing, and draft preparation.
Virendra Kumar Saharan: conceptualization, methodology, and data interpretation
Suja George: supervision, conceptualization, methodology, review, and final draft
All authors read and approved the final manuscript.

Data availability Not applicable.

Declarations

Ethics approval Not applicable.

Consent to participate Not applicable.

Consent for publication Not applicable.

Competing interests The authors declare no competing interests.

References

APHA, AWWA, WEF (2012) Standard Methods for examination of water and wastewater, 22nd edn. Washington: American Public Health Association, pp 1360

Baral SS, Das N, Ramulu TS et al (2009) Removal of Cr(VI) by thermally activated weed Salvinia cucullata in a fixed-bed column. J Hazard Mater 161:1427–1435. https://doi.org/10.1016/j.jhazmat.2008.04.127

Bharathi KS, Ramesh SPT (2013) Fixed-bed column studies on biosorption of crystal violet from aqueous solution by Citrullus lanatus rind and Cyperus rotundus. Appl Water Sci 3:673–687. https://doi.org/10.1007/s13201-013-0103-4

George S, Mehta D, Saharan VK (2020) Application of hydroxyapatite and its modified forms as adsorbents for water defluoridation: an insight into process synthesis. Rev Chem Eng 36:369–400. https://doi.org/10.1515/revce-2017-0101

George S, Bhoi R, Saharan VK (2022) Green biomaterial hydroxyapatite derived from waste marble powder for applications in water defluoridation: comparative study on materials synthesized by different processing routes. Mater Today Proc 57:57–64. https://doi.org/10.1016/j.matpr.2022.01.331

George S, Gupta AB, Mehta M, Goyal A (2021) Pathophysiology of fluorosis and calcium dose prediction for its reversal in children: mathematical modeling, analysis, and simulation of three clinical case studies, 1st edn. Advanced studies in experimental and clinical medicine. Apple Academic Press, pp 195–221. https://www.taylorfrancis.com/chapters/edit/10.1201/9781003057451-13/pathophysiology-fluorosiscalcium-dose-prediction-reversal-children-mathematical-modeling-analysis-simulation-three-clinical-case-studies-suja-george-gupta-mayank-mehta-akshara-goyal

Ghosh A, Chakrabarti S, Biswas K, Ghosh UC (2015) Column performances on fluoride removal by agglomerated Ce(IV)-Zr(IV) mixed oxide nanoparticles packed fixed-beds. J Environ Chem Eng 3:653–661. https://doi.org/10.1016/j.jece.2015.02.001

Khan A, Singh PK, Saharan VK, George S (2020) Synthesis of calcium titanate from marble waste powder for the degradation of congo red dye. Mater Today Proc 43:995–1002. https://doi.org/10.1016/j.matpr.2020.07.620

Khan A, Bhoi RG, Saharan VK, George S (2022) Green calcium-based photocatalyst derived from waste marble powder for environmental sustainability: a review on synthesis and application in photocatalysis. Environ Sci Pollut Res 29:86439–86467. https://doi.org/10.1007/s11356-022-20941-4

Li J, Tian T, Jia Y, et al (2022) Adsorption performance and optimization by response surface methodology on tetracycline using Fe-doped ZIF-8-loaded multi-walled carbon nanotubes. Environ Sci Pollut Res 4123–4136. https://doi.org/10.1007/s11356-022-22524-9

Liang W, Zhan L, Piao L, Rssel C (2011) Fluoride removal performance of glass derived hydroxyapatite. Mater Res Bull 46:205–209. https://doi.org/10.1016/j.materresbull.2010.11.015

Malkoc E, Nuhoglu Y, Abali Y (2006) Cr(VI) adsorption by waste acorn of Quercus ithaburensis in fixed beds: prediction of breakthrough curves. Chem Eng J 119:61–68. https://doi.org/10.1016/j.cej.2006.01.019

Mehta D, Mondal P, George S (2016) Utilization of marble waste powder as a novel adsorbent for removal of fluoride ions from aqueous solution. J Environ Chem Eng 4:932–942. https://doi.org/10.1016/j.jece.2015.12.040

Mehta D, Mondal P, Saharan VK, George S (2017) Synthesis of hydroxyapatite nanorods for application in water defluoridation and optimization of process variables: advantage of ultrasonication with precipitation method over conventional method. Ultrason Sonochem 37:56–70. https://doi.org/10.1016/j.ultsonch.2016.12.035

Mehta D, Mondal P, Saharan VK, George S (2018) In-vitro synthesis of marble apatite as a novel adsorbent for removal of fluoride ions from ground water: an ultrasonic approach. Ultrason Sonochem 40:664–674. https://doi.org/10.1016/j.ultsonch.2017.08.015

Méndez-Lozano N, Apátiga-Castro M, Soto KM et al (2022) Effect of temperature on crystallite size of hydroxyapatite powders obtained by wet precipitation process. J Saudi Chem Soc 26. https://doi.org/10.1016/j.jscs.2022.101513

Mohd Pu'ad NAS, Alipal J, Abdullah HZ et al (2019) Synthesis of eggshell derived hydroxyapatite via chemical precipitation and calcination method. Mater Today Proc 42:172–177. https://doi.org/10.1016/j.matpr.2020.11.276

Saha PD, Chowdhury S, Mondal M, Sinha K (2012) Biosorption of Direct Red 28 (Congo red) from aqueous solutions by eggshells: batch and column studies. Sep Sci Technol 47:112–123. https://doi.org/10.1080/01496395.2011.610397

Sairam Sundaram C, Viswanathan N, Meenakshi S (2009) Fluoride sorption by nano-hydroxyapatite/chitin composite. J Hazard Mater 172:147–151. https://doi.org/10.1016/j.jhazmat.2009.06.152

Scheverin VN, Horst MF, Lassalle VL (2022) Novel hydroxyapatite-biomass nanocomposites for fluoride adsorption. Results Eng 16:100648. https://doi.org/10.1016/j.rineng.2022.100648

Segadães AM, Carvalho MA, Acchar W (2005) Using marble and granite rejects to enhance the processing of clay products. Appl Clay Sci 30:42–52. https://doi.org/10.1016/j.clay.2005.03.004

Singh PK, Saharan VK, George S (2018) Studies on performance characteristics of calcium and magnesium amended alumina for defluoridation of drinking water. J Environ Chem Eng 6:1364–1377. https://doi.org/10.1016/j.jece.2018.01.053

Singh S, Khare A, Chaudhari S (2020) Enhanced fluoride removal from drinking water using non-calcined synthetic hydroxyapatite. J Environ Chem Eng 8:103704. https://doi.org/10.1016/j.jece.2020.103704

Yadav K, Prabhakar R, Jagadevan S (2022) Enhanced defluoridation in household filter using binary metal hydrochar composite. J Clean Prod 370:133525. https://doi.org/10.1016/j.jclepro.2022.133525

Yoon YH, Nelson JH (1984) Application of Gas Adsorption Kinetics I. A theoretical model for respirator cartridge service life. Am Ind Hyg Assoc J 45:509–516. https://doi.org/10.1080/15298668491400197

Zendehdel M, Rezaeian K, Rezaei A, Jalalvandi S (2022) Synthesis and characterization of a low-cost and eco-friendly hydroxyapatite/clinoptilolite/NH2 adsorbent for simultaneous removal of Cr(VI) and F−. SILICON 14:8643–8659. https://doi.org/10.1007/s12633-021-01649-5

Zhang D, Luo H, Zheng L et al (2012) Utilization of waste phosphogypsum to prepare hydroxyapatite nanoparticles and its application towards removal of fluoride from aqueous solution. J Hazard Mater 241–242:418–426. https://doi.org/10.1016/j.jhazmat.2012.09.066